AFRL-AFOSR-JP-TR-2018-0068

Toward High Performance Photovoltaic Cells based on Conjugated Polymers

Yang Yang
UNIVERSITY OF CALIFORNIA LOS ANGELES
11000 KINROSS AVE STE 102
LOS ANGELES, CA 90095-0001

09/19/2018
Final Report

Air Force Research Laboratory
Air Force Office of Scientific Research
Asian Office of Aerospace Research and Development
Unit 45002, APO AP 96338-5002

REPORT DOCUMENTATION PAGE

Form Approved
OMB No. 0704-0188

1. REPORT DATE *(DD-MM-YYYY)*	2. REPORT TYPE	3. DATES COVERED *(From - To)*
20-09-2018	Final	28 Sep 2015 to 27 May 2018

4. TITLE AND SUBTITLE
Toward High Performance Photovoltaic Cells based on Conjugated Polymers

5a. CONTRACT NUMBER

5b. GRANT NUMBER
FA2386-15-1-4108

5c. PROGRAM ELEMENT NUMBER
61102F

6. AUTHOR(S)
Yang Yang

5d. PROJECT NUMBER

5e. TASK NUMBER

5f. WORK UNIT NUMBER

7. PERFORMING ORGANIZATION NAME(S) AND ADDRESS(ES)
UNIVERSITY OF CALIFORNIA LOS ANGELES
11000 KINROSS AVE STE 102
LOS ANGELES, CA 90095-0001 US

8. PERFORMING ORGANIZATION REPORT NUMBER

9. SPONSORING/MONITORING AGENCY NAME(S) AND ADDRESS(ES)
AOARD
UNIT 45002
APO AP 96338-5002

10. SPONSOR/MONITOR'S ACRONYM(S)
AFRL/AFOSR IOA

11. SPONSOR/MONITOR'S REPORT NUMBER(S)
AFRL-AFOSR-JP-TR-2018-0068

12. DISTRIBUTION/AVAILABILITY STATEMENT
A DISTRIBUTION UNLIMITED: PB Public Release

13. SUPPLEMENTARY NOTES

14. ABSTRACT

This is a collaborative research project between Prof. Yang Yang of UCLA and Prof. Kung-Hwa Wei of National Chiao-Tung University in Taiwan on high performance organic photovoltaics. During the three years, they explored several approaches involving advanced ternary blend systems as the active layer, high efficiency charge transport layers and fundamental analysis on polymer:fullerene systems. They significantly improved the OPV efficiency via three different approaches: (a) synthesizing new semiconducting small molecule acceptors and polymer donors in ternary blend systems, (b) employing the new ternary structure and (c) designing new interconnecting layers in tandem OPVs. In addition, the fundamental physics of polymer:fullerene blends was studied to develop and realize strategies to achieve high efficiency devices. As a result, the group achieved tandem devices boasting in excess of 13-14% PCEs by using PBDTTBO as shown in part. The certification of high efficiency devices are under processing by National renewable energy laboratory (NREL).

15. SUBJECT TERMS
Conjugated Polymers, Photovoltaics, Bandgap, Nanocomposites, Interface, Morphology, Nanocrystals

16. SECURITY CLASSIFICATION OF:			17. LIMITATION OF ABSTRACT	18. NUMBER OF PAGES	19a. NAME OF RESPONSIBLE PERSON
a. REPORT	b. ABSTRACT	c. THIS PAGE			WINDER, SHEENA
Unclassified	Unclassified	Unclassified	SAR		19b. TELEPHONE NUMBER *(Include area code)* +81-42-511-2008

Standard Form 298 (Rev. 8/98)
Prescribed by ANSI Std. Z39.18

Final Report to AFOSR

Toward High Performance Photovoltaic Cells based on Conjugated Polymers

Grant Award Number: FA2386-15-1-4108

To: Program Director: Dr. Sheena Winder
Asian Office of Aerospace Research & Development (AOARD)
Air Force Office of Scientific Research (AFOSR)
Tokyo, Japan
(Report coverage: 04/01/2015-05/27/2018)

Prepared by Yang Yang

Department of Materials Science and Engineering

2121C Eng-V Building, UCLA

yangy@ucla.edu

Date: May. 9th, 2018

Towards High Performance Photovoltaic Cells based on Conjugated Polymers

PI: Yang Yang

Department of Materials Science and Engineering

University of California, Los Angeles

Abstract: This is a collaborative research project between Prof. Yang Yang of UCLA and Prof. Kung-Hwa Wei of National Chiao-Tung University in Taiwan on high performance organic photovoltaics. During the three years, we have explored several approaches involving advanced ternary blend systems as the active layer, high efficiency charge transport layers and fundamental analysis on polymer:fullerene systems. The research project was highly productive, publishing 10 papers on journals such as Nature Photonics, Advanced Materials, Advanced Energy Materials, Joule, etc. It is hoped that our work has advanced the development of new organic photovoltaics.

Problem Statement

Through a Taiwan – United States collaboration, we proposed a comprehensive research plan to address the efficiency and manufacturability issues in conjugated polymer solar cells through fundamental studies of material properties, film formation processes and devices. Novel materials and device architectures will be developed to dramatically increase the efficiencies of solution processed single- and multi-junction solar cells. The proposed strategies leverage the advantages of low-cost processing and the uniquely tunable absorption profiles of organic semiconductors, while minimizing charge transport and recombination losses. Therefore, the fundamental research focused on the characterization and modulation of the donor/acceptor interfaces at the nano-scale for providing efficient photo-generation and charge transport in the donor-acceptor blend films. With proper designs of light absorber and interface materials as well as tandem device architectures, we aimed to increase the power conversion efficiencies (PCE) of single junction devices from the current ~10% to 12%, and achieve 15% via multi-junction devices.

Under the previous support of AFOSR, the UCLA team has continuously been a world leader in organic photovoltaics (OPV) and achieved significant progress in morphological understanding and control, interface engineering and novel solution-processed tandem solar cells. This newly collaborated research has brought forth new dimensions in high performance polymers, small molecules, and advanced coating technologies for scalable solar cells. The success of our project is directly correlated with the objectives of the Air Force for flexible, light-weight, and long-lasting power sources for both the Air Force and commercial applications.

Main achievements

1. Unique Energy Alignments of Ternary Material System towards High Performance Organic Photovoltaics (*Advanced Materials*, 30, 1801501 (2018).)

Incorporating narrow bandgap near-infrared absorbers as the third component in donor/acceptor binary blends is a new strategy to improve the PCEs of OPVs. These

near-infrared absorbers can utilize more photons and form a cascade energy heterojunction with donor/acceptor. However, there are two main restrictions: possible charge recombination in the narrow gap material and mis-compatibility between each of the components. The optimized design employs a third component (structurally similar to the donor or acceptor) with a lowest unoccupied molecular orbital (LUMO) energy level similar to the acceptor and a highest occupied molecular orbital (HOMO) energy level similar to the donor. In this design, enhanced absorption of the active layer can be realized without the formation of charge recombination traps and/or interfering with the optimized morphology of the active layer.

In this work, on the basis that ITIC-Th shows a similar backbone and bandgap (1.60 eV), but up-shifted LUMO and HOMO energy levels to IDIC, ITIC-Th was thus chosen as the third component to be added to the binary blend. In order to achieve optimized energy level alignments of ITIC-Th-based third components with the binary blend, ITIC-Th-S and ITIC-Th-O were designed and synthesized through the incorporation of thiophene with alkylthio/alkoxy side chains as a pi-bridge, as shown in **Figure 1**) This approach down-shifts the LUMO energy level and up-shifts the HOMO energy level of the ITIC-Th counterpart and, therefore, red-shifts the absorption into the NIR region (1.45 eV for ITIC-Th-S and 1.40 eV for ITIC-Th-O). Through this chemical modification, the energy levels of ITIC-Th-O were respectively similar to the HOMO energy level of the donor FTAZ (-5.35 eV) and the LUMO energy level of the acceptor IDIC (-3.91 eV).

In summary, through the chemical modifications described above, the HOMO energy levels of the third components were up-shifted to reach that of the donors and the LUMO energy levels of the third components were down-shifted to reach that of the acceptors, keeping in mind that the third components remained similar to the acceptors. Meanwhile, the optimized energy level alignments induce a more efficient charge transfer, which was confirmed by using photoluminescence (PL) scans. Further morphological data were collected by using grazing-incidence wide-angle X-ray scattering (GIWAXS). Due to the similar chemical structures of these third components relative to the acceptors, these materials exhibit good compatibility, such

that the active layers maintained an optimized film morphology at both the molecular and nano scale. As a result, the broadened absorption and enhanced charge transfer contributed to an enhanced short-circuit current (J_{SC}), which are the reasons for the higher performance of the FTAZ/ITIC-Th-O/IDIC ternary system compared with that of a FTAZ/IDIC binary system. The ternary system achieved a PCE of 11.6% compared with a PCE of 10.4% for the binary system, as shown in **Figure 2**.

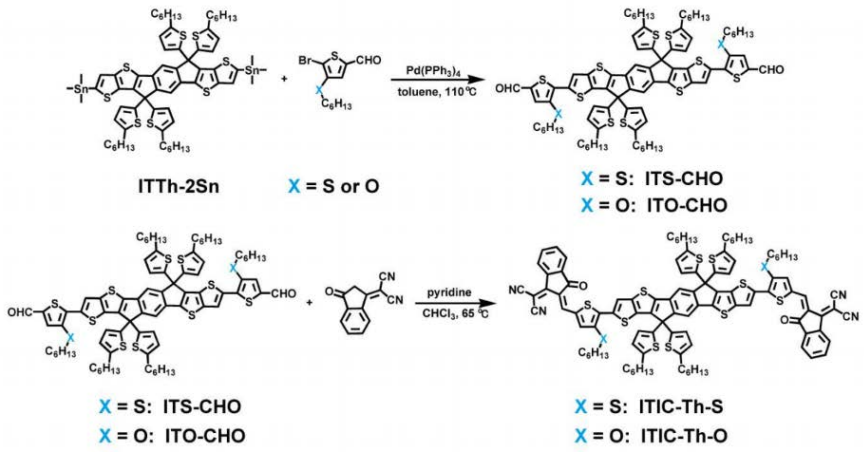

Figure 1. The synthesis routes to synthesize ITIC-Th-S and ITIC-Th-O.

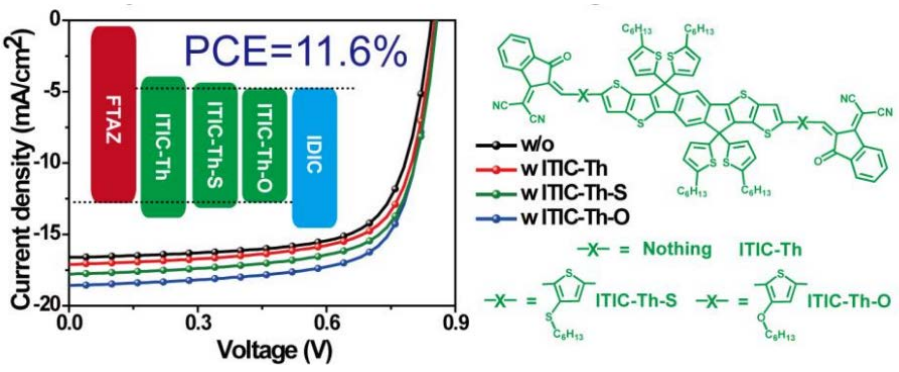

Figure 2. *J–V* curves of devices based on FTAZ/IDIC without or with different third components under illumination of an AM 1.5G solar simulator, 100 mW cm^{-2}.

2. Ternary System with Controlled Structure: A New Strategy toward Efficient Organic Photovoltaics (*Advanced Materials*, 30, 1705243 (2018).)

A new type of active layer with a ternary system has been developed to further enhance the performance of binary system OPV. In the ternary OPV, almost all active layers are formed from simple ternary blends in solution, which eventually leads to the disordered bulk heterojunction (BHJ) structure after a spin-coating process. There are two main restrictions in this disordered BHJ structure to obtain higher performance OPV. One is the isolated second donor or acceptor domains. The other is the invalid metal–semiconductor contact (**Figure 3(a)**).

Herein, the concept and design of donor/acceptor/acceptor ternary OPV with a more controlled structure (C-ternary) is reported. The C-ternary OPV (**Figure 3 (b)**) was fabricated by sequential solution processing in which the third component (the second acceptor) and the binary blend were sequentially spin coated by orthogonal solvents. In order to examine the advantages of this C-ternary structure, the needed fundamental physical properties of the two ternary and one binary system were measured. First, PL quenching efficiency was employed to investigate the charge separation proportions in different films. As shown in **Figure 4 (a)**, the strong PL quenching (94%) of binary and C-ternary films indicates efficient charge separation, while the PL quenching of S-ternary film was relatively low (78%), which might be have resulted from an inefficient charge separation at the interface between the donor and the isolated third component (the second acceptor) domains. Second, space charge limited current (SCLC) method was employed to measure the hole and electron mobilities of the three systems. The hole mobilities and electron mobilities of the binary and C-ternary films were similar, while the S-ternary film exhibited much lower hole mobility (2.0×10^{-4} cm^2 V^{-1} s^{-1}) and electron mobility (7.5×10^{-5} cm^2 V^{-1} s^{-1}) compared to that of the C-ternary film. There are two main factors affecting charge transportation: molecular packing and transportation pathways. The molecular packing of the films was characterized using the GIWAXS patterns. The molecular packing behavior in binary, S-ternary, and C-ternary films were similar in terms of the

polymer crystallite orientation and the $PC_{71}BM$ aggregation. Because of the similarity in molecular packing behavior, the much lower mobility (especially the hole mobility) of the S-ternary film was hypothesized to be caused by the presence of the isolated third component (the second acceptor) domains. These act as traps for charge recombination and restrict the charge transportation pathways. Attributed to higher hole and electron mobility of C-ternary device compared with that of S-ternary device, higher FF (≈70%) can be achieved. To further investigate the charge separation and collection (transportation and extraction) efficiencies in ternary and binary systems, corrected photocurrent measurements were employed as shown in **Figure 4 (b)**. The corrected photocurrent is defined as the device current under illumination as a function of voltage after subtraction of the corresponding dark current ($J_{ph} = J_{light} - J_{dark}$). If the effective applied voltage is large enough, all carriers generated by light absorption in the active layer will be swept out, leading to a saturated current (J_{sat}). The ratio of J_{ph} to J_{sat} represents the product of the charge separation, transportation, and extraction efficiencies. **Figure 4 (b)** shows J_{ph}/J_{sat} for the ternary and binary systems over a range of biases (V_0-V). Compared with the binary device, the S-ternary device exhibited a lower charge separation efficiency and transportation efficiency, which was the reason for the lower J_{ph}/J_{sat} at low electric fields. The J_{ph}/J_{sat} of the C-ternary device at low electric fields was higher than that of the binary device, which was attributed to the enhanced charge extraction efficiency.

After device optimization, the PCEs of all C-ternary devices were enhanced by 14–21% relative to those of the S-ternary blend, as shown in **Figure 4 (c).** The best PCEs were 10.7 and 11.0% for fullerene-based and non-fullerene acceptor solar cells, respectively. The PCE of fullerene-free solar cells was certified by Newport Corporation, yielding a value of 10.32%.

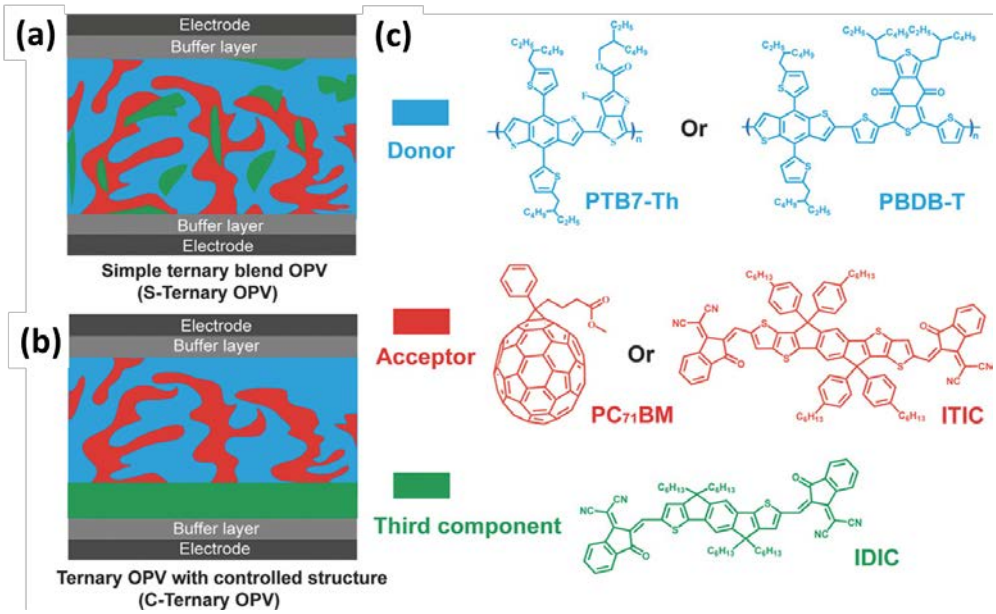

Figure 3. (a) Schematics of S-ternary OPV and **(b)** C-ternary OPV. **(c)** Molecule structures of donors (PTB7-Th, PBDB-T), acceptors ($PC_{71}BM$, ITIC), and the third component (IDIC).

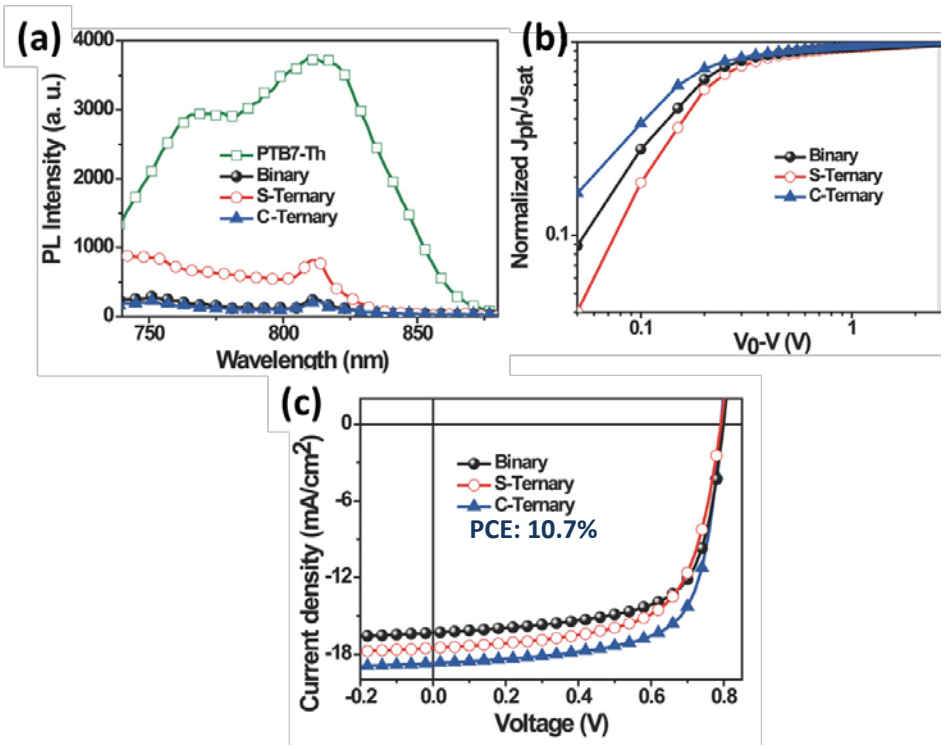

Figure 4. (a) PL and **(b)** corrected photocurrent data as a function of the potential difference V0−V. **(c)** J-V curves of two ternary and one binary PCBM-based systems.

3. Efficient Organic Tandem Solar Cells with Effective Transition Metal Chelates Interconnecting Layer (*Solar RRL*, 1, 1700139 (2017).)

In this work, we demonstrated an efficient tandem solar cell via an efficient tunnel junction (or inter-connecting layer, ICL) with the high efficiency polymer which was synthesized via a collaborative effort between NCTU and UCLA. For developing a stable high-efficiency organic tandem device, besides active materials for sub-cells, one of the most important factors involves the interconnecting layer (ICL), which is indispensable to separate and transport charge carriers from each sub-cell. High quality ICLs are required to have an intact open-circuit voltage (V_{OC}); a tandem OPV without a proper ICL will have a diminished V_{OC} value because of the opposite PN direction for the carriers in the two directly connected sub-cells that have the same anode and cathode on the overall structure. Metal/metal oxide composites have also been adopted due to their good stability and transparency in ICL design. Traditional metal oxide transport layers, however, require a high temperature treatment to increase the number of metal-oxygen bonds in the film so as to obtain good charge carrier mobility. Yet most of the organic photoactive layers experiencing high temperature thermal treatment exhibit severe donor-acceptor phase separation or acceptor recrystallization that lead to stronger charge recombination and smaller photo current.

To enhance the performance of tandem OPVs (device structure shown in **Figure 5 (a)**), we developed a more versatile tunnel junction material, zirconium(IV) acetylacetonate (Zr-acac), as the n-type ICL. Its chemical structure is shown in the inset of **Figure 5 (b)**. The superior electronic and optical properties of Zr-acac enable us to further enhance the performance of each organic sub-cell. The work function of Zr-acac lies above the LUMO levels of the commonly used acceptors. The LUMO levels of the organic-semiconductors will thus be pinned to the Fermi level of the buffer layer, inducing a “barrier free” electron extraction from the LUMOs of the acceptors, which is beneficial for electron transport. The transmittance is higher than the commonly used zinc oxide (ZnO) as shown in **Figure 5 (b)**. Moreover, the

annealing-free process of Zr-acac alleviates the possible damage to the underlying layers during fabrication. In the design of our tandem OPV, we incorporated a large bandgap polymer PBDTTBO (from NCTU group) and a low bandgap polymer PDTP-DFBT (from UCLA group) with $PC_{71}BM$ as the front subcell and rear subcell, respectively. By incorporating Zr-Acac in the ICL of the tandem structure, the performance improved by as much as 20% compared to that using ZnO as ICL. The overall PCE was over 10% while the one of ZnO was 8.4% as shown in **Figure 5 (c)**. From the EQE curves shown in **Figure 5 (d),** it apparently shows that the photocurrent of the tandem OPV with Zr-acac is higher than its counterpart.

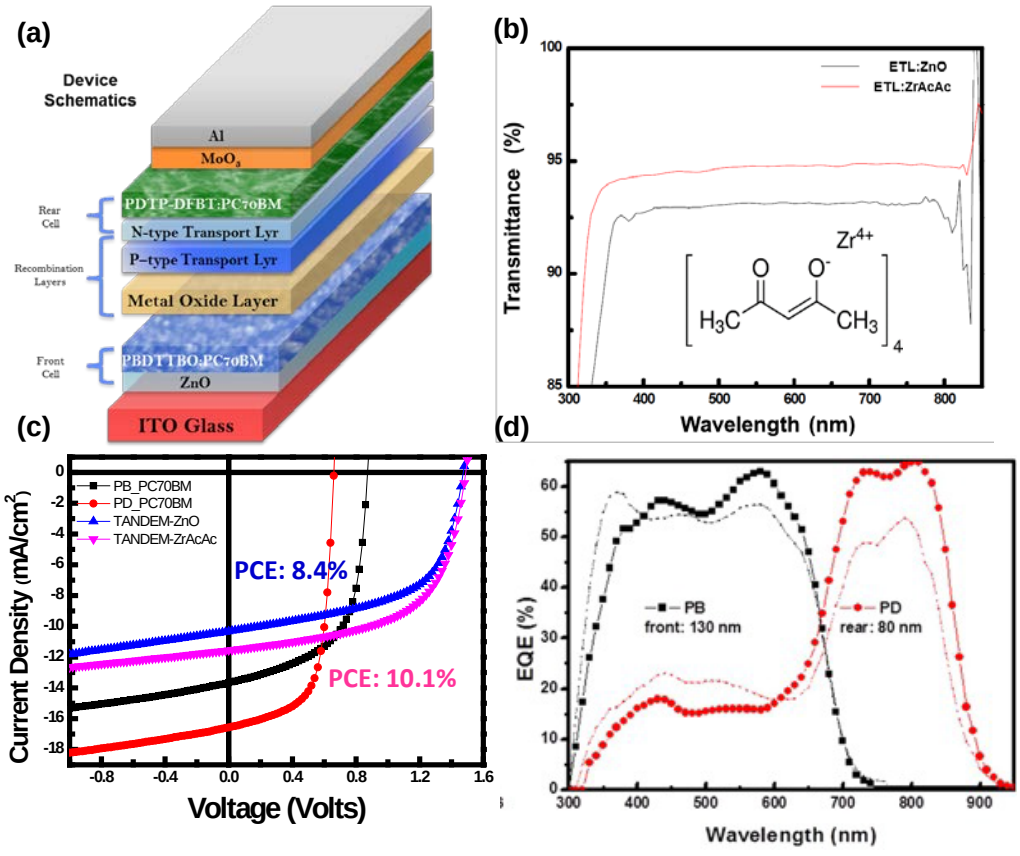

Figure 5 (a) Schematics of PBDTTBO and PDTP-DFBT organic tandem solar cell. **(b)** chemical structure of Zr-acac and transmittance comparison of Zr-Acac and ZnO thin film. **(c)** I-V curve and **(d)** external quantum efficiency of PBDTTBO and PDTP-DFBT single junction and tandem solar cells with ZnO (dashed line) and Zr-Acac (solid line) as interconnecting layer.

4. Influence of Fullerene Acceptor on the Performance, Microstructure, and Photophysics of Low Bandgap Polymer Solar Cells (*Advanced Energy Materials*, 7, 1602197 (2017).)

In this work, the goal was to analyze the thin-film microstructure of polymer/fullerene blends in a bid to achieve higher PCEs. The nano-morphology of polymer/fullerene blends can vary the PCE of an OPV from less than 1% to currently over 11%. Understanding the fundamental science underlying the polymer/fullerene blend is the key to achieve high efficiency OPV devices. However, the resultant microstructure of a film cast from a solution of dissolved donor polymer and acceptor fullerene is very complicated and its analysis is challenging. It is therefore undoubtedly important to establish a systematic method on this issue. To achieve this, the chosen model polymer was a low bandgap polymer, PBDTTT-EFT (also known as PTB7-Th or PCE10), which has been widely used as a reference or a test platform for high efficiency OPV systems. The morphology, photophysics, and device performance of OPVs based on a blend of PTB7-Th with three different fullerene acceptors: $PC_{61}BM$, $PC_{71}BM$, and indene-C60 bisadduct (ICBA) were elaborated.

In order to understand the effect of morphology on device performance, the microstructures of the neat fullerene films and their blends with PBDTTT-EFT were investigated with a combination of synchrotron-based X-ray techniques as shown in **Figure 6 (a)–(c)**. Line profiles of the scattering patterns are plotted in **Figure 6 (d) and (e)**. It was interesting to observe that the intensities of the π–π stacking peak in the $PC_{61}BM$ and $PC_{71}BM$ blends are stronger than that of the ICBA blend, indicating that the polymer π–π stacking is inhibited by the presence of ICBA in the polymer:ICBA blend. In addition, the d-spacings and coherence lengths of the (100) alkyl stacking peak for the three different fullerene blends are summarized in **Figure 6 (f)**. The calculated PBDTTT-EFT (100) d-spacings for the $PC_{61}BM$ and $PC_{71}BM$ blends were higher than the blend with ICBA. Comparing these values, PBDTTT-EFT appeared to be less well-ordered in the PBDTTT-EFT:ICBA blend. To further probe the mesoscale domain structure and purity, resonant soft X-ray

scattering (R-SoXS) was employed, as shown in **Figure 6 (g)**. The Lorentz-corrected scattering profiles for all blends show a well-defined peak, with the peak location associated with a characteristic spacing between fullerene domains. The fitted parameters from the 1D R-SoXS profiles are presented in **Figure 6 (h)**. Among these three blends, the PBDTTT-EFT:$PC_{71}BM$ blend exhibited the largest domain spacing. The domain spacings in the PBDTTT-EFT:$PC_{61}BM$ and PBDTTT-EFT:ICBA blends were both lower. As the domain spacing is proportional to the fullerene domain size, the observed differences in characteristic domain spacing relate to differences in the characteristic domain sizes of these blends. In addition to fullerene domain size, the relative domain purity measured by integrating the total scattering intensity (TSI) also indicated that the blend with $PC_{71}BM$ had the highest domain purity among the three blends. The observed largest domain size and higher domain purity should facilitate charge separation and charge transport.

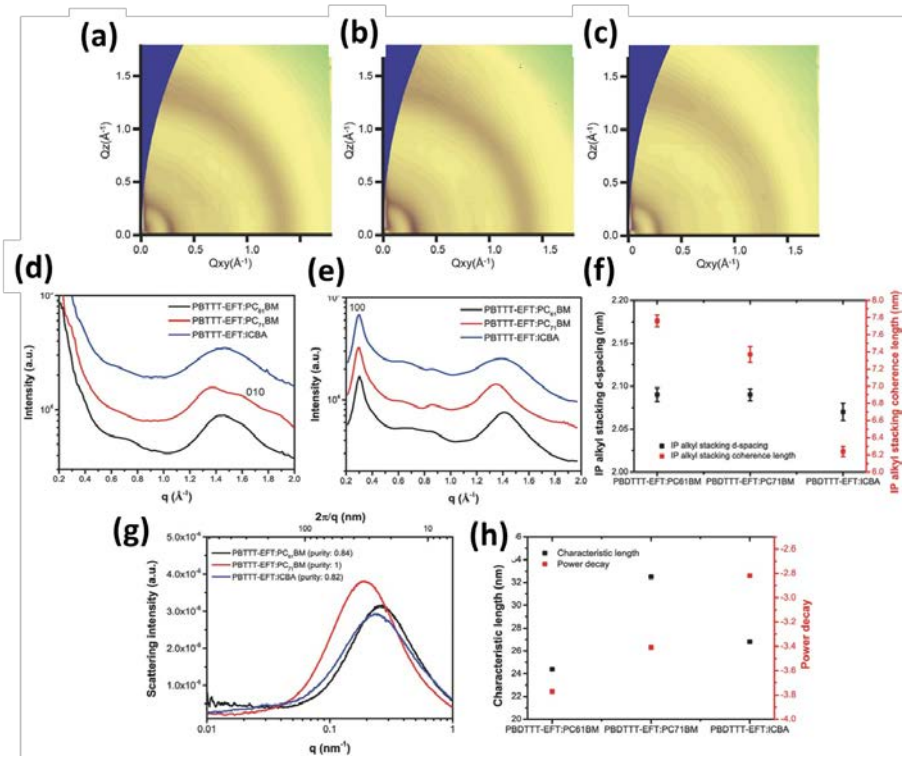

Figure 6 Morphological studies of various polymer:fullerene blends. 2D grazing incidence wide angle X-ray scattering (GIWAXS) patterns of **(a)**

PBDTTT-EFT:$PC_{61}BM$, **(b)** PBDTTT-EFT:$PC_{71}BM$, and **(c)** PBDTTT-EFT:ICBA. Line profiles of various PBDTTT-EFT:fullerene blends cut from 2D GIWAXS patterns: **(d)** out-of-plane (OOP) direction and **(e)** in-plane (IP) direction. **(f)** Lamellar d-spacing and coherence length, determined from the line profiles (e). **(g)** Lorentz-corrected R-SoXS profiles of various PBDTTT-EFT:fullerene blends. **(h)** Fit parameters from R-SoXS scattering profiles.

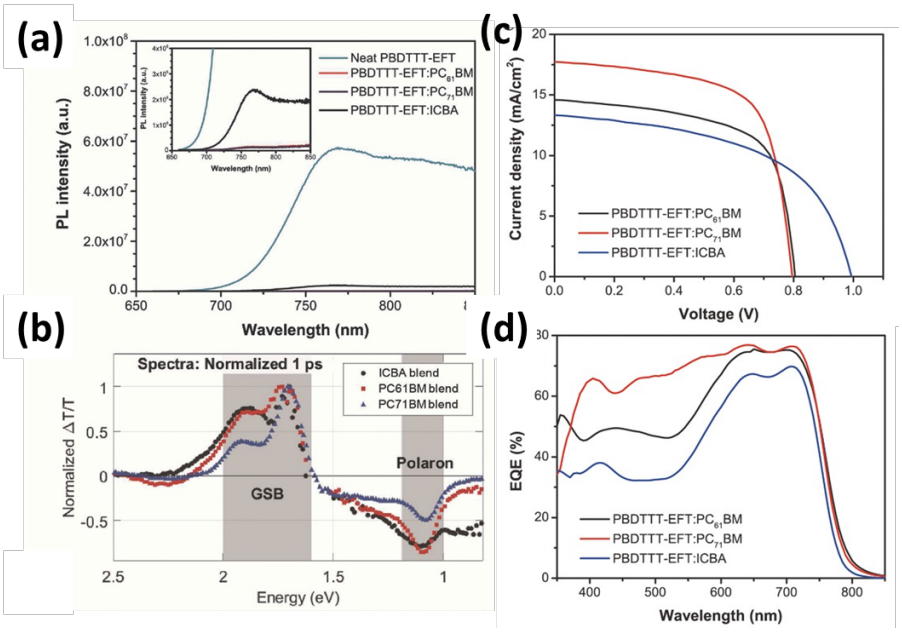

Figure 7 Photophysics studies of the polymer:fullerene blends. **(a)** Steady-state PL spectra of various PBDTTT-EFT:fullerene blends. **(b)** Normalized transient absorption spectra of thin films of PBDTTT-EFT blended with the various fullerene acceptors measured at 1 ps after excitation at 532 nm. The shaded regions represent GSB and polaron features. **(c)** *J–V* curves and **(d)** EQE scans of the polymer:fullerene blends.

In order to establish the relationship between morphology and photophysics, PL spectroscopy and ultrafast transient absorption (TA) spectroscopy were employed to study the charge photogeneration in different blends. **Figure 7 (a)** shows the steady-state PL spectra of neat PBDTTT-EFT and its blends with the different

fullerene acceptors. As the fullerene acceptors were introduced, the photoluminescence was less quenched in the blend with ICBA than in the blends with $PC_{61}BM$ and $PC_{71}BM$. Compared to the other blends, there was a significant fraction of excitons which were not dissociated at a polymer/ICBA interface. The incomplete exciton dissociation in the PBDTTT-EFT:ICBA blend could be attributed to an insufficient driving force (LUMO/LUMO offset) to dissociate all excitons in this blend. To examine the ultrafast dynamics of charge generation and recombination, **Figure 7 (b)** shows normalized TA spectra for the three blends at 1 ps following 532 nmexcitation. The more strongly absorbing $PC_{71}BM$ absorbed the most of the excitation compared with $PC_{61}BM$ and ICBA. The shape of the GSB regions of the 1 ps spectra could be compared to gain some insight into the structure of polymer chains occupied with excitations. The $PC_{71}BM$ blend also had comparatively higher GSB intensity in the 0-0 vibronic band—comparable to the neat polymer. Stronger 0-0 intensity indicates more extended chains, consistent with higher interchain order. In the TA spectra of the ICBA blend, on the other hand, the 0-1 peak approachds the intensity of the 0-0 peak, indicating significant disorder induced by mixing with ICBA, consistent with the GIWAXS measurements discussed above. The TA spectra of the $PC_{61}BM$ blend exhibited an intermediate vibronic ratio and therefore an intermediate level of disruption to polymer packing.

The obtained results were reasonably consistent with the device PCE as shown in **Figure 7 (c) (d)**. Compared to PC_{71} BM-based cells which achieve a power conversion efficiency (PCE) of 9.4% cells using ICBA achieve a higher V_{OC} of 1.0 V due to its energy level matching albeit with a lower PCE of 7.1% because of lower current density and fill factor. In summary, among all three materials, ICBA blends were found to have incomplete PL quenching, lower polymer crystallinity, smaller domain sizes, and less pure phases, attributed to a reduced driving force for phase separation.

5. Energy Transfer Within Small Molecule/Conjugated Polymer Blends Enhances Photovoltaic Efficiency (*J. Mater. Chem. A*, 5, 18053, (2017).)

In this study, we synthesized a small molecule SM-4OMe that has the same BDT units as the polymer PTB7-Th. We only incorporated a small amount of SM-4OMe into the blends for the active layer to ensure the packing of PTB7-Th that is designed for carrier transport is well preserved.

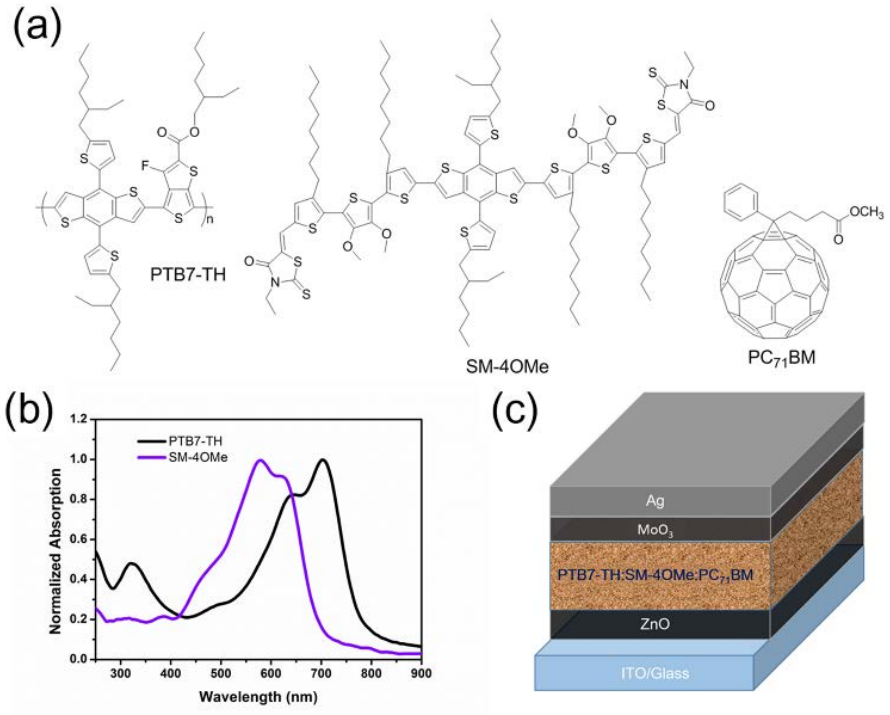

Figure 8 (a) Chemical structures of PTB7-Th, SM-4OMe, and $PC_{71}BM$; **(b)** UV–Visabsorption spectra of films of PTB7-Th and SM-4OMe. **(c)** Inverted device structure.

Figure 8 (a) presents the chemical structures of PTB7-Th, SM-4OMe, and $PC_{71}BM$; Fig. 1b displays the UV–Vis absorption spectra of PTB7-Th and SM-4OMe in the form of solid films. The absorption ranges of SM-4OMe and PTB7-Th film extended from 400 to 700 nm and from 500 to 800 nm, respectively; their complementary absorption of their blends ensured a broader absorption spectrum (from 400 to 800 nm). Thus, we suspected that devices incorporating ternary blends of PTB7-Th, SM-4OMe, and $PC_{71}BM$ as active layers would be highly likely to

display increased photocurrents, relative to those of corresponding device incorporating only binary blends of either PTB7-Th or SM-4OMe with $PC_{71}BM$, under the condition that carrier transport are similarly effective in both cases.

Figure 9 (a) displays the UV–Vis absorption spectra of films of SM-4OMe and PTB7-Th, as well as the PL spectrum of the film of SM-4OMe. The UV–Vis absorption spectrum of PTB7-Th overlaps with the PL spectrum of SM-4OMe in the range from 660 to 810 nm, indicative of possible energy transfer from SM-4OMe to PTB7-Th. **Figure 9 (b)** and **c** show the PL spectra of binary and ternary blend films incorporating various weight ratios of SM-4OMe, respectively. **Figure 9 (b)** displays that for the binary blend films when the amount of SM-4OMe increases, both the sharp peak at 690 nm and the broad peak from 720-860 nm that result from SM-4OMe become stronger, although at different extent. Whereas, for the ternary blend films, the PL peak was severely quenched for the cases of incorporated SM-4OMe being less than 20%.

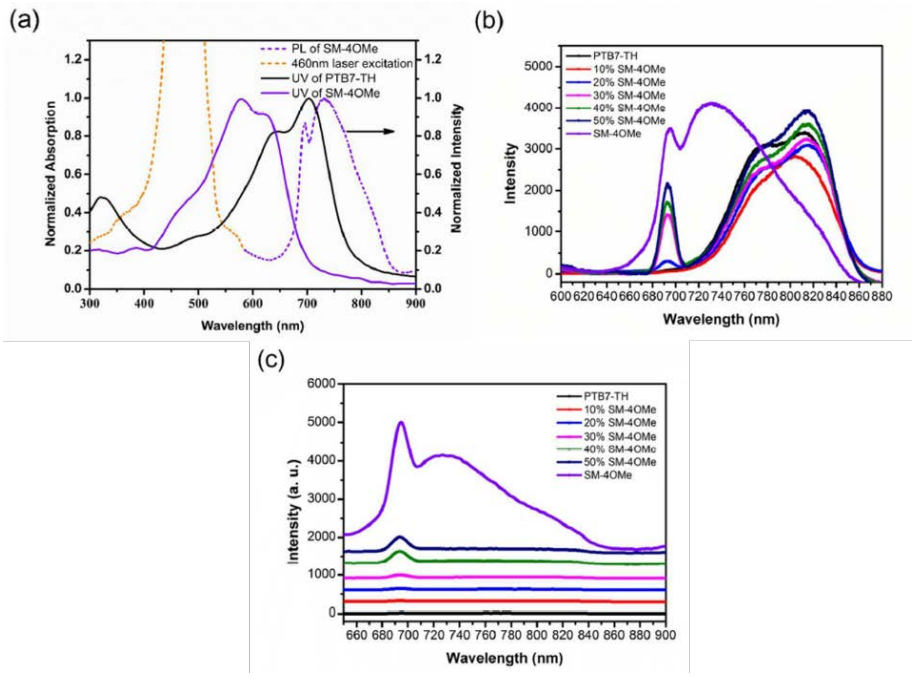

Figure 9 (a) UV–Vis absorption spectra of films of SM-4OMe and PTB7-Th and PL spectrum of a film of SM-4OMe. PL spectra of solid films incorporating various

weight ratios of SM-4OMe: **(b)** binary and **(c)** ternary blends [$PC_{71}BM$ blend ratio = 1:1.5 (w/w); processed with 2 vol% DIO].

The PCE of a device incorporating a ternary blend of PTB7-Th:SM-4OMe:$PC_{71}BM$ as the active layer increased to 10.4% from a value of 8% for the corresponding device incorporating PTB7-Th:PC71BM—a relative increase of 30%. This enhancement resulted from energy transfer from the high band gap small molecule SM-4OMe to the low band gap polymer PTB7-Th, owing to the affinity between the small molecule and the polymer that have a similar chemical structure unit benzodithiophene and their optimized phase-separated morphology that is comprised of smaller and more fullerene clusters and slightly better polymer lamellae packing that provide more pathways for carriers transport. This approach enhances the absorption of the solar spectrum and, thus, the PCE of single-junction polymer photovoltaics.

6. Molecular engineering of side chain architecture of conjugated polymers enhances performance of photovoltaics by tuning ternary blend structures (*Nano Energy*, 43, 138, (2018).)

In this study, we propose a systemic way of tuning the morphology of ternary blends through molecular engineering of the donor (D) chemical units and the side chain architecture of the acceptor (A) chemical unit of a synthesized donor-acceptor (D/A) conjugated polymer to influence the packing of another D/A conjugated polymer that has a complementary band gap for enhancing their carrier transport. Here, we systematically engineered the side chains of the conjugated polymer PBDTTBO and studied its interactions with the polymer PTB7-Th, which has the same BDTT donor chemical unit, in ternary blends, also including a fullerene, as the active layer for photovoltaics.

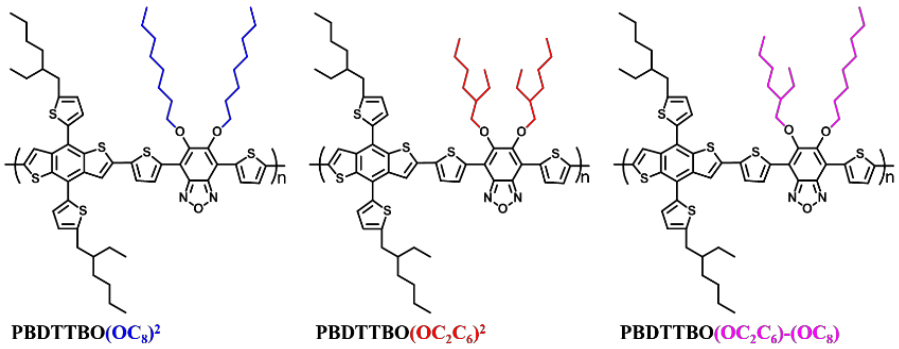

Figure 10. Chemical structure of the copolymers PBDTTBO(OC8)^2, PBDTTBO(OC_2C_6)^2, and PBDTTBO(OC_2C_6)-(OC_8).

Figure 10 presents the chemical structures of the three tested polymers—PBDTTBO(OC_8)^2, PBDTTBO(OC_2C_6)^2, and PBDTTBO(OC_2C_6)-(OC_8)—with different side chain architectures. They all feature the same donor unit, bis[5-(2-ethylhexyl)thien-2-yl]benzodithiophene(BDTT), which is also present in PTB7-Th, to enhance the interactions between PBDTTBO and PTB7-Th through, presumably, π-stacking of BDTT units in the ternary blend active layers. The three PBDTTBO polymers differ in terms of the side chains—two linear, two branched, or mixed linear-and-branched alkoxy units—on their benzo[c] [1,2,5] oxadiazole (BO) units. PBDTTBO(OC_8)^2 has two linear chains attached to the BO unit, PBDTTBO(OC_2C_6)^2 has two branched chains, and PBDTTBO(OC_2C_6)-(OC_8) has one linear and one branched side chain, randomly distributed along the BO units. We incorporated each of these three polymers as the second component, blended with PTB-TH and $PC_{71}BM$, to fabricate ternary blend inverted devices in a quest to enhance the PCEs over those of the corresponding PTB7-Th:$PC_{71}BM$ binary blend cell devices.

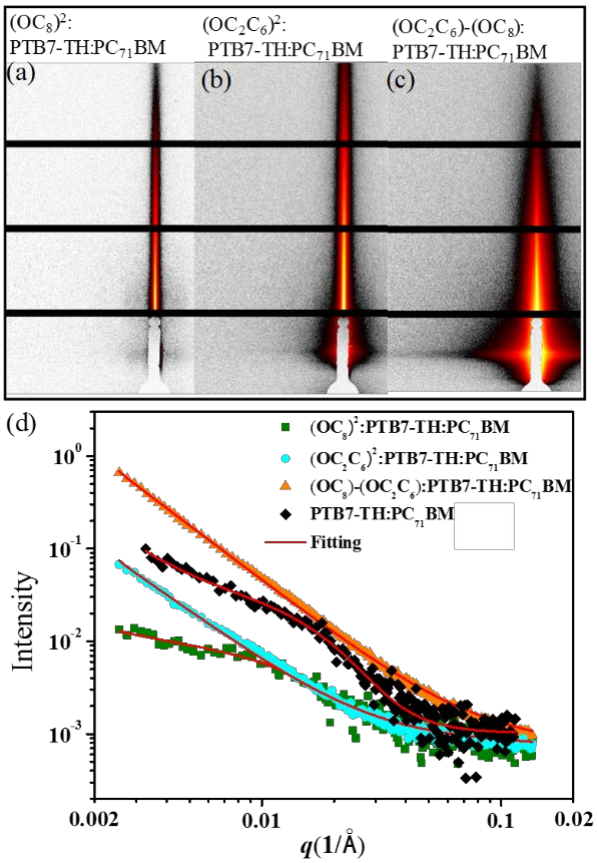

Figure 11. (a–c) 2-D GISAXS patterns of the ternary blends (a) $(OC_8)^2$:PTB7-TH:$PC_{71}BM$, (b) $(OC_2C_6)^2$:PTB7-TH:$PC_{71}BM$, and (c) (OC_2C_6)-(OC_8):PTB7-TH:$PC_{71}BM$. (d) Corresponding 1-D line-cut profiles.

To further explain this phenomenon, we carried out 2-D GISAXS analyses. We found that the $(OC_2C_6)^2$: PTB7-Th:$PC_{71}BM$ ternary blend film contained the smallest $PC_{71}BM$ clusters (2.0 nm) and a greater quantity of clusters dispersed in the blend film, thereby providing more pathways between clusters for electron transport to the electrode and resulting in the highest PCE of 11.4%.

Through rational structural side chain modification of the donor-acceptor conjugated polymers, the resulting PCE of the branched PBDTTBO/PTB7-Th /PC71BM ternary blend device increased to 11.4% from 9.0% for the corresponding PTB7-Th /PC71BM binary blend device, highlighting the importance of careful selection of appropriate side chain structures when incorporating efficient D–π–A third-component polymers in ternary blend solar cells. Enhanced interaction between

the branched PBDTTBO and PTB7-Th make this system an ideal candidate for use in ternary blend solar cells.

7. Review Articles

We contributed four review articles on prestigious journals including Nature Review Materials, Advanced Materials, Nature Photonics and Joule.

(1) Low-Bandgap Conjugated Polymers Enabling Solution-Processable Tandem Solar Cells. Gang Li, Wei-Hsuan Chang and Yang Yang. Nature Reviews Materials 2(8), 17043 (2017)

(2) High-Performance Organic Bulk-Heterojunction Solar Cells Based on Multiple-Donor or Multiple-Acceptor Components. Wenchao Huang, Pei Cheng, Yang (Michael) Yang, Gang Li, Yang Yang. Advanced Materials, 30, 1705706 (2018).

(3) Next-Generation Organic Photovoltaics Based on Non-Fullerene Acceptors. Pei Cheng, Gang Li, Xiaowei Zhan and Yang Yang. Nature Photonics, 12 (3), 131 (2018).

(4) Transparent Polymer Photovoltaics for Solar Energy Harvesting and Beyond. Sheng-Yung Chang, Pei Cheng, Gang Li and Yang Yang. Joule, in press (2018).

Conclusions and Outlook

In summary, over the past three years, this project has been considerably fruitful. We have significantly improve the OPV efficiency via three different approaches: (a) synthesizing new semiconducting small molecule acceptors and polymer donors in ternary blend systems, (b) employing the new ternary structure and (c) designing new interconnecting layers in tandem OPVs. In addition, the fundamental physics of polymer:fullerene blends have also been studied to develop and realize strategies to achieve high efficiency devices. As a result, our group has achieved tandem devices boasting in excess of 13-14% PCEs by using PBDTTBO as shown in part. The certification of high efficiency devices are under processing by National renewable energy laboratory (NREL). Exciting progress has been made by our group under the

support of AFOSR, which paves the way for future academic and commercialization breakthroughs.